

A monolithic tunable symmetric bistable mechanism

Hussein Hussein¹, Fahimullah Khan¹ and Mohammad I. Younis¹

¹ Physical Sciences and Engineering Division, King Abdullah University of Science and Technology, Thuwal 23955-6900, Saudi Arabia

E-mail: Mohammad.Younis@kaust.edu.sa

Received xxxxxx

Accepted for publication xxxxxx

Published xxxxxx

Abstract

A tunable symmetric bistable micro-machined mechanism with monolithic structure is presented. The mechanism consists of two sets of pre-shaped beams of similar properties and dimensions; however with one set is curved opposite to the other. The bistability is induced by creating a negative stiffness behavior at the initial position of the moving part to break its stability. This is possible at a certain electrothermal axial loading of both beam sets. The active bistability is symmetric with respect to the initial position. The distance between stable positions is tunable with the applied electrothermal voltages. The mechanism can be used as a tunable bi-directional actuator with different applied voltages. The design and concept are demonstrated based on finite-element simulations and experimental measurements.

Keywords: bistable mechanism, symmetric snap-through, tunable bistability, monolithic structure.

1. INTRODUCTION

Buckled and pre-shaped beams are widely used as bistable mechanisms at the small and large scale [1]. These mechanisms are employed in various applications in many sectors, including soft robotics [2], metamaterials [3], multistable positioning [4,5], resonators [6,7], actuators [8], gas sensing [9], pressure sensing [10], threshold sensing [11,12], logics [13], space applications [14], biomedical [15], and energy harvesting [16,17].

These mechanisms are attractive due to their many advantages, such as simplicity, small footprint, monolithic and compliant structures, passive holding, low actuation energy, large deformations at small forces and within elastic limits, energy storage, eliminating friction and backlash, and negative stiffness behavior.

The buckled beam configuration is mainly obtained by axial compression. The snap-through behavior of post-buckled beams is symmetric between the two sides of buckling. This results in non-conditional bistability. In

contrast, pre-shaped beams are easier to be implemented in monolithic structures, where there is no need for axial compression. However, due to their shifted initial state, the initial stable side has more margin of stability, while the second stable position exists under some conditions [18–20].

Buckled and pre-shaped beams are known for having a negative stiffness behavior in their snap-through zone of deflection. This is necessary condition for bistability. A negative stiffness behavior means that the restoring force of the moving part decreases with further displacement. Electrothermal axial actuation of a beam can result in enlarging the negative stiffness zone of deflection.

In this paper, we present a tunable symmetric bistable mechanism with a monolithic structure. The concept is based on breaking the stability of the moving part at the as-fabricated position to create bistability.

The mechanism consists of two sets of pre-shaped beams, curved opposite to each other, with the same properties and dimensions. The opposite beams are connected to a shuttle at their mid-length. In the passive state (without axial load), this

creates a high rigidity relatively characterizing the lateral displacement of the shuttle.

Axial and lateral forces between the two inverted beams sets are induced via electrothermal Joule's heating of the beams using the same voltage load. Due to the similarity between the opposite beams, the shuttle initial position (zero displacement) remains at a zero force position after applying the same voltage load on both sides. The initial position becomes unstable at a certain level of heating, since the shuttle lateral stiffness becomes negative. This leads to bistability.

The design of the bistable mechanism ensures a symmetrical snap-through behavior; the snapping force variation with the shuttle displacement is equivalent in both lateral directions. Hence, in the bistability conditions, the distance from the initial to the two stable positions is equal and is tunable with the electrical inputs. Further, the mechanism can be used as a bidirectional actuator by differentiating the electrical inputs on the opposite beams.

The rest of the paper is organized as follows. The snap-through behavior of pre-shaped beams is described in Section 2. The creation of a negative stiffness behavior at the initial position by electro-heating the pre-shaped beams is described in Section 3. The concept of the tunable bistable mechanism is presented in Section 4. Experiments on micro-fabricated prototypes of the tunable bistable mechanism are presented in Section 5. Advantages, limitations, and potential applications of the proposed mechanism are discussed in Section 6.

2. SNAP-THROUGH OF PRE-SHAPED BEAMS

The parallel configuration of pre-shaped beams contains several beams with similar shape and dimensions connected to a shuttle at their mid-length as shown in figure 1. Compared to a single beam, the parallel configuration prevents the activation of the anti-symmetrical modes of buckling. This enhances the bistability of the pre-shaped beams and constrains a linear snap-through displacement of the shuttle [20]. The most common shapes of pre-shaped bistable beams mechanisms are the curved and inclined shapes [20].

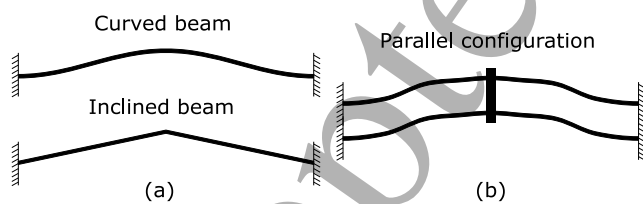


Figure 1. Single (a) and parallel (b) configurations of pre-shaped beams.

Pre-shaped beams are used in microelectromechanical systems (MEMS) due to their ease of fabrication without the need of external forces or hinged boundaries to induce buckling. However, their snap-through behavior is not ideally symmetric between the two sides of buckling. A symmetrical snap-through behavior results in a non-conditional bistability

and similar margin of stability between the two sides of buckling. Pre-shaped beams with variable cross-section were designed to enhance the symmetry in the snap-through behavior [21–24]. The symmetry indicates that the switching force is similar in the forward and backward directions. This is practical for applications where the same conditions are required from the two stable sides. Besides, the symmetry allows designing a robust bistable mechanism, even with very small distance between stable positions.

Figure 2 shows the typical snapping force curve for a pre-shaped bistable curved beam. The snapping force f is the actuating lateral point force applied to the shuttle; its magnitude is equivalent to the static restoring force of the beams at the midpoint with an opposite direction. The force and displacement direction and the dimensional parameters are clarified in figure 3. The existence of positive and negative snapping force indicates bistability; the beam is pushing towards the other side of buckling after certain level of deflection. The bistability for pre-shaped beams exists after some level of the initial height to thickness ratio h/t [20].

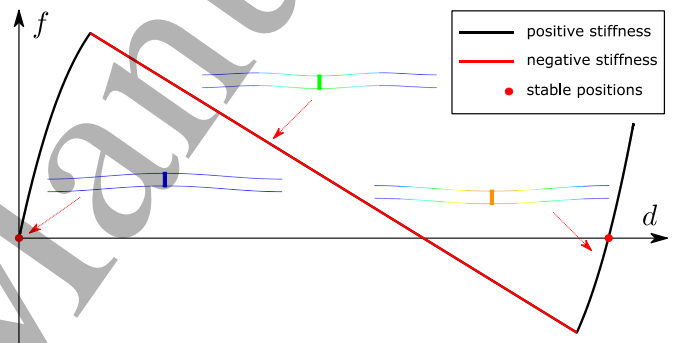


Figure 2. Snapping force curve of a bistable pre-shaped beam.

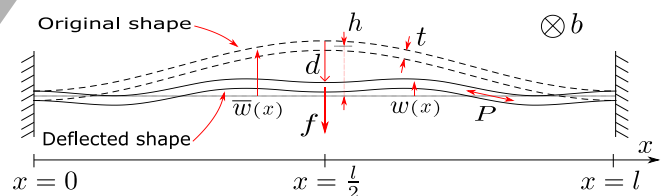


Figure 3. Schematic of a pre-shaped curved beam.

A stable position has two essential properties: zero snapping force ($f = 0$) indicating the absence of restoring force at this position, and a positive stiffness behavior ($\frac{\partial f}{\partial a} > 0$). In the distance between the two stable positions of a bistable structure, the beams are more axially compressed ($P > 0$). This results in a negative stiffness behavior ($\frac{\partial f}{\partial a} < 0$) after some limits of axial compression [20]. The intermediate negative stiffness zone is necessary for the existence of two stable positions. Considering parallel configuration, in which two beams are connected by a shuttle in the middle, the axial compression is capped by the third critical load ($P = P_3$) [20].

At this limit, the third mode of buckling appears in the beam shape, resulting in a linear negative stiffness behavior ($\frac{\partial f}{\partial d} = c < 0$, c is a constant) as shown in figure 2.

In this work, we are interested in extending the range of negative stiffness behavior to reach the initial position ($d = 0$). This is possible with electrothermal heating as clarified in the next section.

3. SNAP-THROUGH OF ELECTRO-THERMAL ACTUATORS

Parallel pre-shaped beams are used also as electro-thermal actuators. The bistable beam dimensions are chosen usually to enhance the bistability [25] (distance between stable positions, holding forces, miniaturization, etc.), while the beam actuator dimensions are chosen to maximize the actuator output (free and loaded displacement) [26]. Figure 4 shows schematics of a curved beam actuator in different states: in the initial state (figure 4.a), with electrical activation and free load (figure 4.b), with a point load (figure 4.c), and with the third mode of buckling considering parallel configuration and excessive point load (figure 4.d).

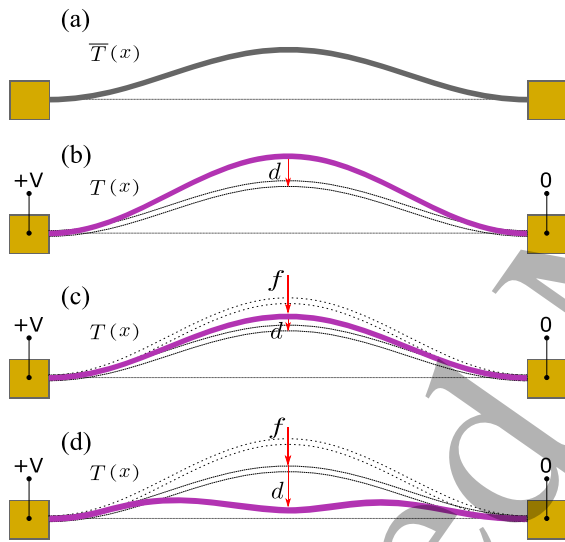


Figure 4. Configurations of an electrothermal curved actuator at rest (a), after electrothermal heating (b), with a pushing point load (c), and with the third mode of buckling due to an excessive load (d).

The electrothermal heating results in an expansion of the beam length, due to the induced axial compression load. The structure of the beam amplifies the length expansion (which is usually small) to a larger lateral displacement d . At free load, the thermal expansion moves up the beam mid-point ($d < 0$) and extends the snapping zone of the beam. Figure 5 shows the snapping force curve of a pre-shaped curved beam with and without electrothermal heating.

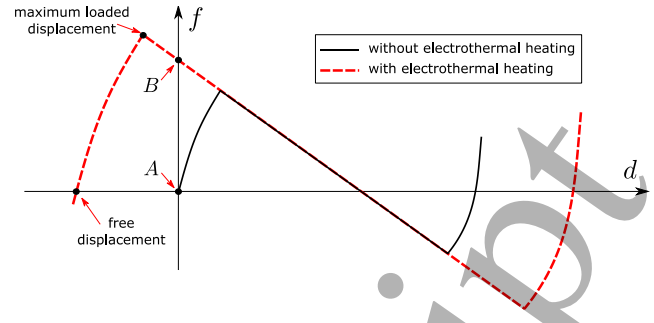


Figure 5. Snapping force of a pre-shaped curved beam with and without electrothermal heating. Points A and B are at the initial position of both snapping force curves.

The third mode of buckling is still activated with electrothermal heating at the critical load. The resulting negative stiffness with the third mode of buckling keeps the same value (negative force curve slope) as shown in figure 5. The negative stiffness behavior helps snapping to the other stable position, and hence enhances bistability. However, buckling at the third mode is not desirable for electrothermal actuators since the negative stiffness limits their capacity to push higher loads.

The snapping zone (including negative stiffness zone) extends continuously with the applied voltages. After some voltage limit, the stiffness at initial position ($d = 0$) becomes negative as the case presented in figure 5 (point B). The bistable mechanism presented in this paper is based on the creation of a negative stiffness behavior at the initial position to break its stability and create a tunable bistability.

4. A TUNABLE SYMMETRIC BISTABLE MECHANISM

The tunable symmetric bistable mechanism presented in this paper consists of two opposite sets of pre-shaped beams with similar material and dimensions. The two opposite sides are connected to the same shuttle at their mid-length as shown in figure 6.

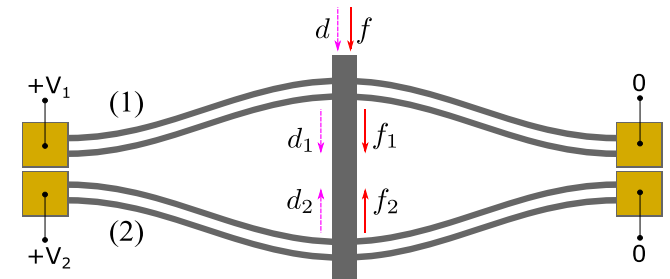


Figure 6. Tunable symmetric bistable device.

Let d_1 , f_1 , d_2 , f_2 , d , and f be the lateral deflection and snapping force of sets 1 and 2 and their combinations, respectively. The deflection parameters (d_1 , d_2 , d) are positive when the shuttle moves in the same arrows direction (i.e. downwards for d and d_1 and upwards for d_2), and are negative in the other direction. Similarly, the force parameters

(f_1, f_2, f) are positive when the snapping force is applied to the shuttle in the same arrows direction, and are negative in the other direction. The connection of inverted beams to the same shuttle imposes the following displacement constraint:

$$d = d_1 = -d_2 \quad (1)$$

The snapping forces vary with the applied voltages and deflection. The snapping forces f_1 and f_2 are related to the total snapping force f as follows:

$$f(V_1, V_2, d) = f_1(V_1, d) - f_2(V_2, d) \quad (2)$$

Considering the same applied voltages ($V_1 = V_2 = V$), the similarity between the two opposite sets of pre-shaped beams imposes the following constraint in terms of snapping forces:

$$f_1(V, d) = f_2(V, -d) \quad (3)$$

Substituting (3) into (2), we notice the symmetry of the total snapping force with respect to the initial position:

$$f(V, V, d) = -f(V, V, -d) \quad (4)$$

The symmetric property in (4) indicates the zero snapping force at the initial position:

$$f(V, V, 0) = 0 \quad (5)$$

Hence, for the same voltage difference applied on both sides, the initial position is a stable position as long as the lateral stiffness around it is positive ($\frac{\partial f}{\partial d}(V, V, 0) > 0$). At low voltages, both set of beams show positive stiffness behavior at the initial position as explained in the previous section. After some voltage, each set of beams shows negative stiffness behavior at the initial position, which results in a total negative stiffness ($\frac{\partial f}{\partial d}(V, V, 0) < 0$). Inducing the negative stiffness in this way breaks the stability of the initial position and leads to bistability. Figure 7 shows the total snapping force curve in the case where each set of the opposed pre-shaped beams has the same snapping force curve of the example presented in figure 5 with electrothermal heating.

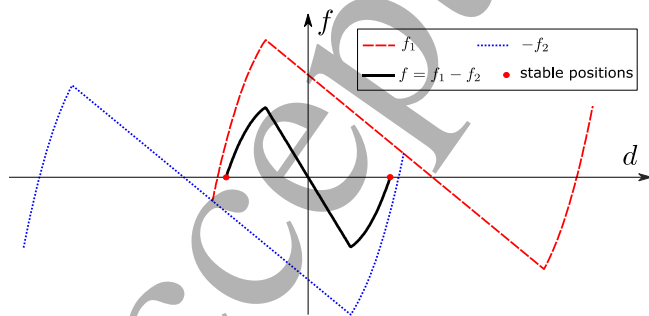


Figure 7. Total snapping force for the tunable symmetric bistable device.

In case of bistability, the total snapping force symmetry with respect to the initial position (4) provides the same margin of stability between the two stable sides. This is a main advantage with respect to the shifted and conditional bistability of preshaped beams. The case shown in figure 7 is for one voltage V that is higher than the critical voltage of bistability. Figure 8 shows the variation of the total snapping force curve for different applied voltages.

The curves in figure 8 are calculated with finite element (FE) simulations for a device similar to figure 6 with the following dimensions for each beam: $l=2$ mm, $t=9.2$ μm , $h=13.2$ μm , and $b=25$ μm . The material properties for a doped silicon are considered (resistivity ρ_0 : 0.124 Ω mm, Young's modulus E : 169 GPa, density ρ : 2.32 g cm^{-3} , thermal conductivity K_p : 149 $\text{W m}^{-1} \text{K}^{-1}$, specific heat C_p : 706 $\text{J Kg}^{-1} \text{K}^{-1}$, and temperature dependent thermal expansion coefficient α [27]). These parameters result in good agreement with the experimental measurements as shown in the next section.

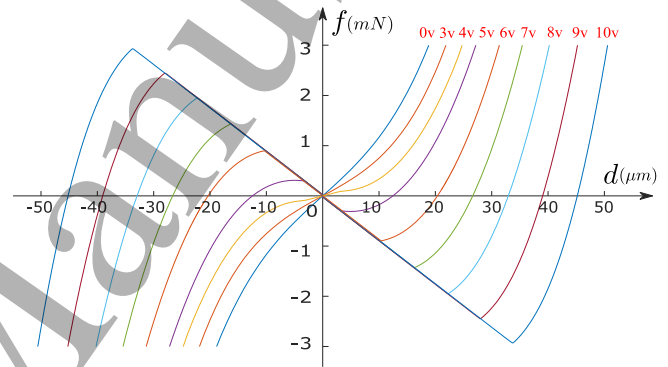


Figure 8. Simulated curves of snapping force versus deflection for the tunable symmetric bistable device with various electrothermal voltage loads V .

Finite element simulations have been used to obtain the snapping force curves in figure 8. The element type "plane223" is used in the FE software Ansys with structural-thermoelectric static analysis. Up to $V=4$ v, the simulations are simply made by firstly increasing the voltage with small steps while fixing the shuttle, then, at the voltage level, the shuttle is moved with small steps and the snapping forces are obtained. For higher voltages, where the negative stiffness and third mode of buckling start to occur, the first scenario makes divergence. The scenario in this case is to move the shuttle to one side at zero voltage, increases the voltages and then moves back the shuttle with small steps. Constraining the symmetry with respect to the beams mid-length reduces the problems of divergence in the simulations.

At zero voltage, the mechanism is stiff against lateral displacement of the shuttle. The stiffness revealed by the lateral stiffness (slope of snapping force curve) at the initial position starts to decrease after applying voltages as shown in figure 8. After a critical voltage limit, the lateral stiffness becomes negative and two stable positions are induced. At higher voltage, the distance between stable positions increases

as the snapping zone is expanding. Figure 9 shows variation of the stable positions of the mechanism at different voltages.

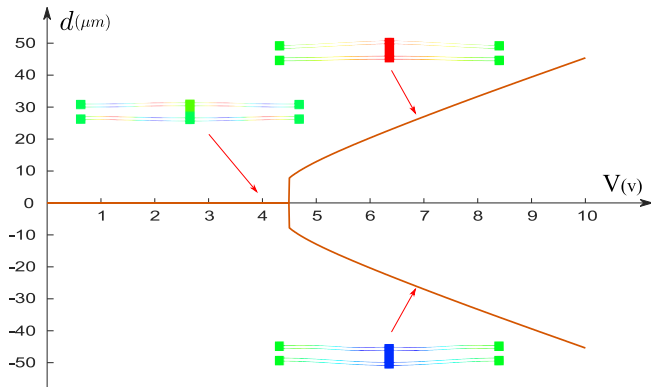


Figure 9. Stable positions for the tunable symmetric bistable device with various voltages V .

The snapping force around the critical voltage is highly sensitive to voltage and displacement variation, as shown in figure 9. This high sensitivity is suitable for sensing applications, where materials with biological, chemical or physical dependent properties can be used. Further, the restoring forces in this zone of voltage (around the critical voltage) is limited to a certain extent, which allows a near zero-force displacement behavior.

Furthermore, the bistable mechanism can be used as a bidirectional actuator by differentiating the voltages applied on the two beam sets. A close configuration for a bidirectional actuator is reported in [28], where Z-shaped beams are used due to their similar lateral stiffness in the two directions of motion. The working principle is to activate one side to make a motion or to push loads, while keeping the other side inactivated. The actuator in this case has low stiffness and limited force capabilities due to the opposite internal forces between both sides. The electrothermal heating reduces the lateral stiffness of one beam actuator at its initial position as explained previously. Hence, activating both sides of the mechanism with different voltages results in an improved actuating performance in the two directions of motion.

These applications are not investigated in this paper. Nevertheless, the bidirectional actuation is used in the experiment, as shown in the next section, to choose the stable side after applying voltages. Activating the beams in one side slightly before those in the other side favors switching the shuttle to one stable side rather than the other.

5. EXPERIMENTAL MEASUREMENTS

The theoretical concept of the tunable symmetric bistable mechanism is tested experimentally on microfabricated prototypes. The prototypes are fabricated on SOI wafers (25 μm device layer) using SOI-MUMPsTM fabrication process through MEMSCAP [29]. The beam dimensions measured after fabrication are the same considered for the FE

simulations in figures 8 and 9, except for the length, which is 1 mm. In the previous section, we choose to present the simulation for larger length to show that this reduces the critical voltage of bistability due to the increase in the beam length expansion (i.e. more axial load at the same voltages). Further, changing the length does not change the maximum temperature reached at the same voltages (to a large extent), as shown later in this section. This indicates that the range of bistability for the mechanism with acceptable temperature limits can be increased by increasing the length.

The prototypes are tested on-wafer using Cascade Microtech's Summit 12000 AP semi-automatic probe station, as shown in figure 10.

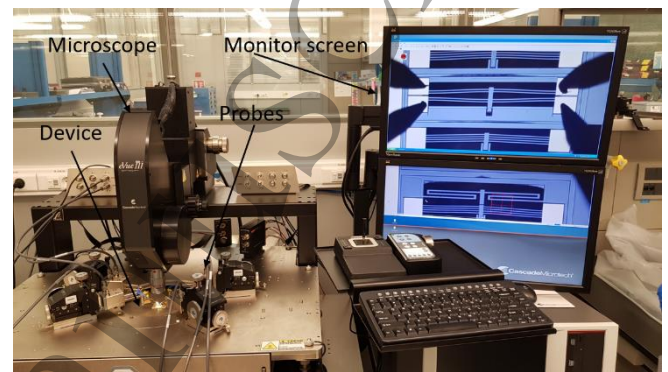


Figure 10. Experimental setup.

The voltages are applied through probes using a programmable power supply (keysight E36234A) allowing coupled outputs with delays. The voltages are applied on the pads as clarified in figure 6 with a delay between V_1 and V_2 . For low voltages below the critical voltage of bistability, the triggering order between V_1 and V_2 is not important since the beam will come back to the initial position after activating both voltages. In case of bistability at higher voltages, activating V_1 slightly before V_2 switches the shuttle to the top stable side, while inverting the sequence order switches the shuttle to the bottom stable side. Figure 11 shows the switching sequence in both cases. A small delay of several milliseconds is enough to favor the displacement in one direction. We considered a delay of 0.5s in the experiments.

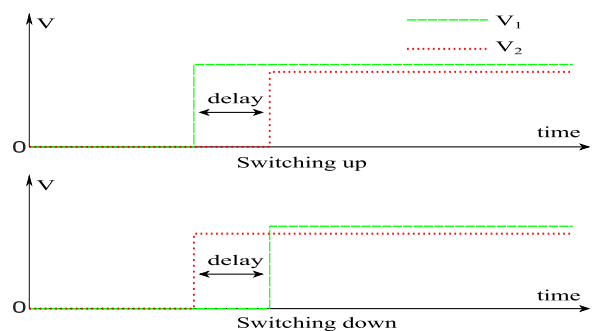


Figure 11. Voltage sequence to switch up or switch down.

The mechanism shuttle displacement is measured using the camera software. Figure 12 shows the bistable mechanism before and after applying voltages on the pads with a zoom on the shuttle at initial, top, and bottom positions.

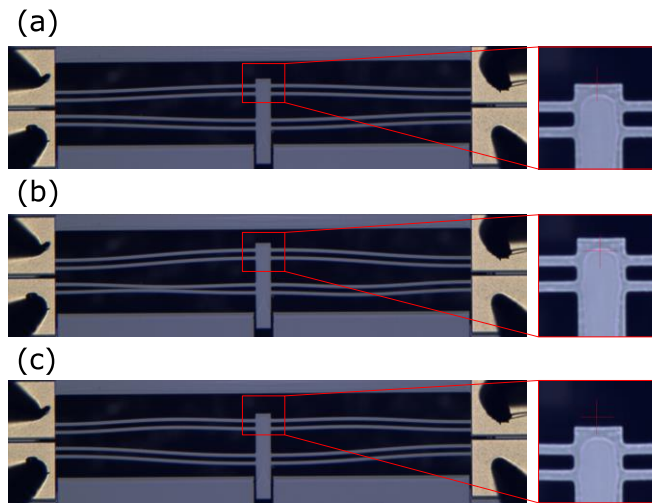


Figure 12. The bistable device at (a) zero voltage, (b) the upper, and (c) bottom stable positions at high voltages.

The experimental tests were carried out on several prototypes with the same dimensions. Very close behavior is shown between the different prototypes. Table I shows the displacement measurements of the bistable mechanism for different applied voltages. The measurements validate the concept of the bistable mechanism. At voltages below 4 v, the displacement is very small, even when activating only one side. For voltages up to 8 v, the shuttle comes back to the initial position after activating both sides. The critical voltage of bistability is between 8 v and 8.5 v (V_2). At $V \approx V_2=8.5$ v, a huge snap of the shuttle to top or bottom positions is noticed relatively to a small voltage variation. Afterwards, the distance to stable positions increases for higher voltages.

Table 1. Experimental displacement measurements on the fabricated prototype in response to electrical inputs.

Voltage (v)		Displacement (μm)
V_1	V_2	
4.1	4	0
5.2	5	
6.4	6	
7.7	7	
8	7.5	
8.6	8	
9	8.5	
9.3	8.75	-10.4
9.5	9	+11.7
		-11.9
		+12.4
		-12.7

The concept of the tunable symmetric bistable mechanism is based on applying the same voltage difference on both opposite pre-shaped beam sets. The small difference in voltages experimentally is set to calibrate both sides to have the same force-displacement behavior, as much as possible. This difference could be attributed to the difference in cable and probe contact resistances or some microfabrication imperfections. The experimental measurements show good agreement with FE simulations as shown in figure 13.

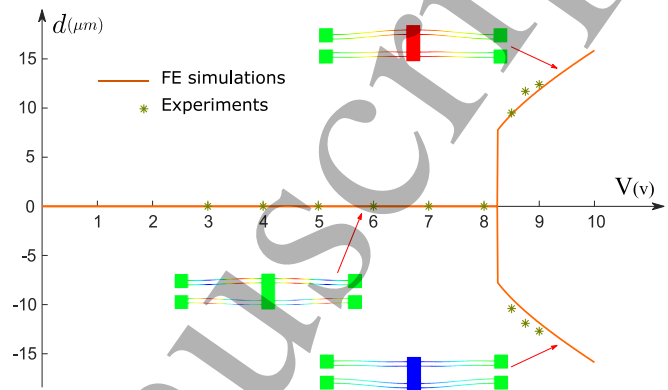


Figure 13. Comparison of stable positions between FE simulations and experiments.

As shown in figure 13 and noticed experimentally, the mechanism displacement at the critical voltage of bistability (near 8.4 V) is very sensitive to the applied voltages. Slightly before the critical voltage, we notice a weak equilibrium of the mechanism at the initial position, where the shuttle is sensitive to external disturbances like vibration. Above the critical voltage, the distance between stable positions increases with more voltages. However, in the fabricated prototypes, the range of bistability is very limited where the bistable mechanism shows failure due to the high temperature level after 10 V. Further, we notice that the mechanism changes its properties or shape plastically after working at high temperature for long time. This is revealed by a shifting of the critical voltage of bistability to a higher level.

6. ADVANTAGES, LIMITATIONS, AND POTENTIAL APPLICATIONS

The tunable bistable mechanism shows several advantages, making it promising for different applications. It has a simple and monolithic structure. This simplifies the design, fabrication, and integration of the mechanism with other MEMS structures for more complicated functions. The tunable bistable mechanism has a symmetrical snap-through behavior and bistability, while not requiring special mechanisms to induce buckling, such as external axial forces, moveable boundaries, or initial activation [30].

The symmetry makes the proposed mechanism beneficial for bistable mechanism applications, since there is no need to

deal with different holding/switching conditions at each stable position.

The holding and switching at and between stable positions are essential functions for the functioning of bistable and multistable devices. The holding in the proposed mechanism relies on the elastic stability of the structure, at different levels of electro-thermal heating, between the two lateral sides. The switching of bistable mechanisms is usually carried using additional actuators pushing the moving part to switch between stable positions. In the proposed mechanism, the switching can be made using the mechanism itself with no need for external actuators. Switching is achieved by electro-thermally activating/de-activating the beams, in each of the opposite sides, one before the other.

The tunability is an additional advantage of the proposed mechanism compared to other bistable mechanisms. It can be used for applications where the stable position needs to be tuned or set at very small or very large distance with respect to dimensions. The holding/snapping forces can be tuned as well between the two sides of stability. This is helpful for applications where the snap-through is used as indicator for reaching a threshold limit of a physical quantity, such as acceleration or flow. The tunability in this case helps to increase the range of sensing and its accuracy.

Further, the displacement at the critical voltage of bistability is very sensitive for small variations in the electrical input. Using a beam material sensitive for a physical stimulus, such as humidity, temperature, gas concentration, the shift in the critical voltage can be used for sensing applications.

Furthermore, the snapping forces around the critical voltage of bistability are very small (see figure 8). This helps to extend the range of displacement with small restoring forces. Due to symmetry, the proposed mechanism has a zero force and negative stiffness behavior at the initial position, in the bistability conditions. Thus, adding this mechanism to an equivalent positive stiffness mechanism (such as a cantilever beam, a spring, etc.) cancels out the opposite restoring forces and makes a near zero-force displacement mechanism.

The tunable bistable mechanism can be used also as a bidirectional actuator by differentiating the electrical inputs on the two opposite beam sets. Each of the opposite beam sets acts as a beam electrothermal actuator (like a V-shape). Applying voltages to one beam set in one side separately moves the middle shuttle towards that side and deflects the beams in the other side in their range of snap-through.

The opposite configuration of the proposed mechanism has an advantage of compensating the effects of residual stresses after fabrication. The residual stresses will make an expansion of each beam, which is similar to the effect of electrothermal heating. The residual stress would be the same in the different beams, as they have the same material and dimensions. This results in zero displacement at the middle shuttle due to the

opposite configuration. This is helpful as well to reduce the critical voltage limit for the proposed mechanism.

In terms of performance, the force and distance between stable positions of the tunable bistable mechanism increase with the applied voltages. The maximum voltage that can be applied, without failure or plastic deformation, is limited by two main constraints: temperature and stress limits.

The maximum variation of temperature ΔT_{max} (with respect to initial temperature) in a slender pre-shaped beam due to the application of a voltage difference ΔV between its anchors can be approximated with the following expression:

$$\Delta T_{max} = \frac{\Delta V^2}{8\rho_0 K_p} \quad (6)$$

The expression of ΔT_{max} in (6) is calculated based on the electro-thermal heat equation with constant thermal properties and neglected convection and radiation. It shows that the temperature reached in the beam for a certain voltage is independent from the beam dimensions. Figure 14 shows a comparison between FE simulations and the analytical expression in (6) for the maximum temperature reached at different voltages. The same material properties and dimensions (with two different lengths) as the previous simulations are considered in figure 14.

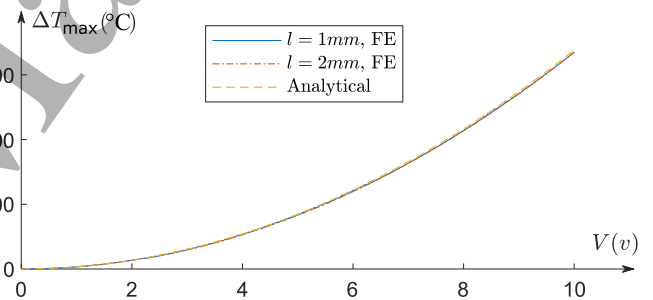


Figure 14. The maximum temperature reached in the beams at different voltages between FE simulations and analytical calculations.

The axial and bending stresses increase in the pre-shaped beams of the bistable mechanism with higher voltages and with lateral deflection. Figure 15 shows variation of the maximum internal stresses in the proposed mechanism obtained with FE simulations (same material properties and dimensions as previously). For a fair comparison, the voltages in figure 15 are chosen differently (with different beam length) to obtain approximately the same distance between stable positions. Note that the stress in pre-shaped beams increases with higher thickness and smaller length [19].

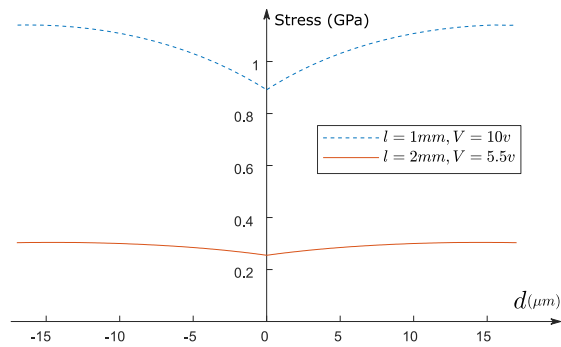


Figure 15. The maximum stress reached in the beams at different voltages.

The temperature and stress limit for the material have to be considered as constraints in the design of the tunable bistable mechanism. Considering these limits with safety factors enhances the design robustness. For silicon, the fracture occurs at 2 GPa stress or higher at room temperature [31,32]. The fracture limit depends on many parameters, including fabrication conditions, crystallographic orientation, geometry, temperature, etc. [33]. Silicon properties vary with the temperature and degrade permanently at high temperatures. Silicon electrothermal actuators remain functioning properly for temperature up to 650 °C. The strength of silicon and its fracture limit reduce at elevated temperature [34]. A failure stress around 0.8 GPa at temperature of 800 °C is measured on polysilicon structures in [34].

The tunable bistable mechanism with 2mm length has a low critical voltage of bistability, and a wider working range at low for the tunable bistable mechanism temperature and smaller stresses. Accordingly, a design issue is to lower the critical voltage and increase the range of tunable force and displacement, while adhering to temperature and stress limits.

The opposite forces applied by the opposite beams in the tunable bistable mechanism increase the level of stress inside the shuttle. The shuttle dimensions need to be large enough to support these stresses. In addition, the shuttle and the distance between beams must be large enough to constraint the rotation of the shuttle and ensure a straight displacement. Otherwise, the tunable bistable mechanism will switch between stable positions with tilted configurations. This is because the second mode of buckling with rotation at the mid-point (constrained by the shuttle) is easier to occur with less deformation energy than in the case of the third mode of buckling [18,19].

The concept of the proposed mechanism is based on applying equally voltage difference on each of the opposite sides of the mechanism. However, a small difference in voltages is set experimentally between the two sides to calibrate a symmetrical snap-through behavior. A remaining challenge is to compensate the difference in the applied voltages on fabricated prototypes to induce symmetric bistability. In addition, developing analytical models for the mechanism is helpful for a better understanding of its behavior, optimising its performance, and tuning the different properties for various applications.

7. CONCLUSION

The concept, design, and experiments on a tunable symmetric bistable mechanism with monolithic structure are presented. The bistability of the mechanism is based on creating a negative stiffness in the initial position to break its stability. Electro-thermal heating of pre-shaped beams is used to create the negative stiffness behavior at the initial position of the moving part. The symmetry of the mechanism is a main advantage with respect to the bistability of pre-shaped beams. The symmetry is obtained using similar pre-shaped beams, which are opposite to each other and heated with the same voltages. The distance between the stable positions is tunable with the applied voltages. The concept was demonstrated based on FE simulations and experiments, which are in very good agreement. The new mechanism opens the path for promising applications: tunable bistability, bidirectional actuator with more powerful scheme of voltage control, sensing applications, near zero-force mechanism, resonators, etc. Further, the principle of creating bistability by creating a negative stiffness at the initial position can be generalized to other domains, at other scales, and with different tools.

Acknowledgements

This research is supported by KAUST research fund.

References

- [1] Hu N and Burgueño R 2015 Buckling-induced smart applications: recent advances and trends *Smart Mater. Struct.* **24** 063001
- [2] Rafsanjani A, Bertoldi K and Studart A R 2019 Programming soft robots with flexible mechanical metamaterials *Sci. Robot.* **4** eaav7874
- [3] Kadic M, Milton G W, van Hecke M and Wegener M 2019 3D metamaterials *Nat. Rev. Phys.* **1** 198–210
- [4] Hussein H, Bouhadda I, Mohand-Ousaid A, Bourbon G, Le Moal P, Haddab Y and Lutz P 2018 Design and fabrication of novel discrete actuators for microbotic tasks *Sensors Actuators, A Phys.* **271** 373–82
- [5] Liu X, Lamarque F, Doré E and Pouille P 2015 Multistable wireless micro-actuator based on antagonistic pre-shaped double beams *Smart Mater. Struct.* **24** 075028
- [6] Hajjaj A Z, Jaber N, Ilyas S, Alfosail F K and Younis M I 2020 Linear and nonlinear dynamics of micro and nano-resonators: Review of recent advances *Int. J. Non. Linear. Mech.* **119** 103328
- [7] Roozbahani M M, Moghimi Zand M, Mousavi

- Mashhadi M, Dehghan Banadaki M, Jafari Ghalekohneh S and Cao C 2019 Dynamic pull-in instability and snap-through buckling of initially curved microbeams under the effect of squeeze-film damping, mechanical shock and axial force *Smart Mater. Struct.* **28** 097001
- [8] Zhang J, Wu Z, Zhang C, Hao L, Nie R and Qiu J 2019 Nonlinear dynamics of shape memory alloys actuated bistable beams *Smart Mater. Struct.* **28** 055009
- [9] Jaber N, Ilyas S, Shekhah O, Eddaoudi M and Younis M I 2018 Smart Gas Sensing and Actuation Using Multimode of a MOFs Coated Microbeam 2018 *IEEE SENSORS* (IEEE) pp 1–4
- [10] Hajjaj A Z, Chappanda K N, Batra N M, Hafiz M A A, Costa P M F J and Younis M I 2019 Miniature pressure sensor based on suspended MWCNT *Sensors Actuators A Phys.* **292** 11–6
- [11] Ramini A, Younis M I and Su Q T 2013 A low-g electrostatically actuated resonant switch *Smart Mater. Struct.* **22** 025006
- [12] Frangi A, De Masi B, Confalonieri F and Zerbini S 2015 Threshold Shock Sensor Based on a Bistable Mechanism: Design, Modeling, and Measurements *J. Microelectromechanical Syst.* **24** 2019–26
- [13] Hafiz M A A, Kosuru L and Younis M I 2016 Microelectromechanical reprogrammable logic device *Nat. Commun.* **7** 11137
- [14] Zirbel S A, Tolman K A, Trease B P and Howell L L 2016 Bistable mechanisms for space applications ed M S Kellermayer *PLoS One* **11** e0168218
- [15] Salem M Ben, Aiche G, Rubbert L, Renaud P and Haddab Y 2018 Design of a Microbiota Sampling Capsule using 3D-Printed Bistable Mechanism *Proceedings of the Annual International Conference of the IEEE Engineering in Medicine and Biology Society, EMBS* vol 2018-July pp 4868–71
- [16] Vysotskyi B, Parrain F, Aubry D, Gaucher P and Lefeuvre E 2016 Innovative Energy Harvester Design Using Bistable Mechanism With Compensational Springs In Gravity Field *J. Phys. Conf. Ser.* **773** 012064
- [17] Safaei M, Sodano H A and Anton S R 2019 A review of energy harvesting using piezoelectric materials: state-of-the-art a decade later (2008–2018) *Smart Mater. Struct.* **28** 113001
- [18] Qiu J, Lang J H and Slocum A H 2004 A curved-beam bistable mechanism *J. Microelectromechanical Syst.* **13** 137–46
- [19] Hussein H, Le Moal P, Bourbon G, Haddab Y and Lutz P 2015 Modeling and Stress Analysis of a Pre-Shaped Curved Beam: Influence of High Modes of Buckling *Int. J. Appl. Mech.* **07** 1550055
- [20] Hussein H and Younis M I 2019 Analytical study of the snap-through and bistability of beams with arbitrarily initial shape *J. Mech. Robot.* **12** 1–21
- [21] Chen Q, Zhang X, Zhang H, Zhu B and Chen B 2019 Topology optimization of bistable mechanisms with maximized differences between switching forces in forward and backward direction *Mech. Mach. Theory* **139** 131–43
- [22] Gao R, Li M, Wang Q, Zhao J and Liu S 2018 A novel design method of bistable structures with required snap-through properties *Sensors Actuators A Phys.* **272** 295–300
- [23] Huang Y, Zhao J and Liu S 2016 Design optimization of segment-reinforced bistable mechanisms exhibiting adjustable snapping behavior *Sensors Actuators A Phys.* **252** 7–15
- [24] Tran N D K and Wang D-A 2017 Design of a crab-like bistable mechanism for nearly equal switching forces in forward and backward directions *Mech. Mach. Theory* **115** 114–29
- [25] Hussein H, Le Moal P, Younes R, Bourbon G, Haddab Y and Lutz P 2019 On the design of a preshaped curved beam bistable mechanism *Mech. Mach. Theory* **131** 204–17
- [26] Wittwer J W, Baker M S and Howell L L 2006 Simulation, measurement, and asymmetric buckling of thermal microactuators *Sensors Actuators A Phys.* **128** 395–401
- [27] Okada Y and Tokumaru Y 1984 Precise determination of lattice parameter and thermal expansion coefficient of silicon between 300 and 1500 K *J. Appl. Phys.* **56** 314–20
- [28] Zhu Y, Moheimani S O R and Yuce M R 2012 Bidirectional Electrothermal Actuator With Z-Shaped Beams *IEEE Sens. J.* **12** 2508–9
- [29] Cowen A, Hames G, Monk D, Wilcenski S and Hardy B 2002 *SOIMUMPs design handbook*
- [30] Hussein H, Khan F and Younis M I 2020 A symmetrical bistable mechanism from combination of pre-shaped microbeams *Sensors Actuators A Phys.*
- [31] McLaughlin J C and Willoughby A F W 1987

1
2
3 Fracture of silicon wafers *J. Cryst. Growth* **85** 83–90
4

5 [32] LaVan D, Jackson K, McKenzie B, Glass S,
6 Friedmann T, Sullivan J and Buchheit T 2008 Direct
7 Tension and Fracture Toughness Testing Using the
8 Lateral Force Capabilities of a Nanomechanical Test
9 System *Mechanical Properties of Structural Films*
10 (ASTM International) pp 62-62–10

11 [33] DelRio F W, Cook R F and Boyce B L 2015
12 Fracture strength of micro- and nano-scale silicon
13 components *Appl. Phys. Rev.* **2** 021303
14

15 [34] Boyce B L, Grazier J M, Buchheit T E and Shaw M
16 J 2007 Strength distributions in polycrystalline
17 silicon MEMS *J. Microelectromechanical Syst.* **16**
18 179–90
19
20
21
22
23
24
25
26
27
28
29
30
31
32
33
34
35
36
37
38
39
40
41
42
43
44
45
46
47
48
49
50
51
52
53
54
55
56
57
58
59
60